

Optimal Wave Drag Reduction Technique for Fighter Aircraft Using von Kármán Ogive & Haack Series

Habiba Jamal, Syed M. Farhan Naveed, M. Zain Javed, Muneeb Ahsan, Shuaib Salamat

Aerospace Engineering Department, Air University, Pakistan

Corresponding author: Zain Javed (e-mail: zain@aerospace.pk).

Abstract— In the supersonic regime, total drag rises colossally at higher speeds due to shockwaves. Drag reduction is imperative for modern fighter aircraft to efficiently sustain higher Mach during flight. Hence, various techniques are integrated into the preliminary design phase enabling these modern fighter aircraft to super-cruise. Area ruling leads to better high-speed aerodynamic performance. Utilizing the Sears-Haack cross-sectional area ruling techniques is one of the drag-minimization processes. Various Haack series are explored in this study for a wing-body configuration to analyse the methodology that can be applied for the design of a modern multi-role fighter aircraft ensuring the required aircraft volume is conserved. Application of Von Kármán integral equation leads to better optimization of fuselage shape and hence impart a significant effect on supersonic drag. Employing this phenomenon, in the following research, decreased wave drag by 45% at Mach 1.0. Other Haack series can provide better results but the implementation is limited by the area of application. Therefore, the selection of methodology applied for the enhancement of supercruise capability is the key finding of this study.

Keywords— Aerodynamic efficiency, Area rule, Far-field theory, Haack series, Optimisation, Supersonic flight, Wave drag

I. INTRODUCTION

Wave drag and aerodynamic efficiency are the measures of the performance of aircraft. Especially in the case of modern fighter aircraft where high speed is an essential characteristic of the performance profile. The measure of aerodynamics can be estimated through the maximum lift to drag ratio or fuel consumption.

Drag produced by the aircraft during its flight determines the aerodynamic efficiency of the aircraft. Greater the speed requirement, the greater the drag penalty. Whereat higher speeds, the drag shoots up because of wave drag contribution to the total drag. Therefore, this increase in drag at higher speeds experienced by the aircraft deteriorates the operational effectiveness of the aircraft. The theory of wave drag extends to the phenomenon of energy transfer from the supersonic aircraft to the surrounding air as strong shock waves. The formation of shockwaves is uniquely associated with the high-speed aerodynamics as the pressure drag increases and dominates the transonic and supersonic flight regimes. Due to this particular aerodynamics constraint and the urge to make modern fighters as competent as possible in terms of maximum speed, different theories and experiments have been carried out for the reduction of wave drag. Wave drag is highly dependent on the geometry of the aircraft and flight conditions. Geometrical parameters with maximum impact are the volume and the cross-sectional area distribution of the aircraft. To solve the consequence of geometry and its effect on the aerodynamics, supersonic area rule is used in the conceptual design and optimization of high-speed aircraft.

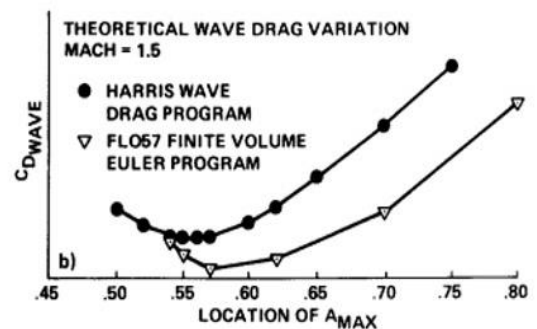


Figure 1 - Wave drag relative to the location of the maximum cross-sectional area for selected STOVL and conventional fighters [1]

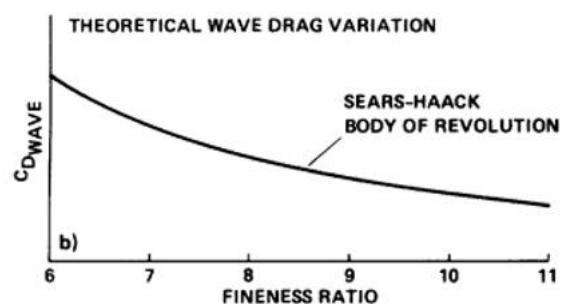


Figure 2 - Wave drag relative to fineness ratio for selected STOVL and conventional fighters [1]

Wave drag variation with the location of the maximum cross-sectional area is studied, as shown in Figure 1[1] implying that the lowest wave drag is obtained when the maximum area is located at 50-60% along fuselage length

from the nose. According to various research works, the fineness ratio contributes significantly to wave drag. For a Sears Haack body, wave drag decreases when the fineness ratio is increased as shown in Figure 2. The relationship between aircraft geometry and wave drag is far more complex. For the past seven decades, interest is shown in the methodology of reducing wave drag due to the quest to manufacture aircraft with high supersonic speed capabilities. Today, the requirement of a supersonic dash is converted into super-cruise. One of the factors contributing to this capability of next-generation fighter aircraft is slender bodies with reduced drag. Raptor, Gripen, or Rafale, all latest aircraft are designed upon the very methodology of area ruling.

A. Harris Wave Drag Code

A linearized aerodynamic code is used to estimate the supersonic wave drag component of the total drag which itself is based on the area rule method. This phenomenon is based on the fact that the measure of wave drag is dependent upon the shape of the fuselage, which means that the change in the area encountered by flow in the longitudinal direction determines how much wave drag does the body produces when travelling at a supersonic speed.

Hence, refined volume distribution of the body longitudinally is required for the reduction of wave drag which can be attained by correct placement and arrangement of volumetric components. Von Karman slender body formula is applied to the equivalent bodies for the estimation of wave drag. The calculation is an accumulated integral of all the sections.

B. Supersonic Area Ruling

The supersonic area rule works by passing a series of cutting planes along the longitudinal axis of the aircraft as shown in Figure 3. The cutting planes are inclined at the Mach angle μ with respect to the x-axis of the aircraft. This set of cutting planes can be orientated at different angles of rotation (θ) about the aircraft roll axis to approximate the Mach cone. The equivalent body area at each station is projected on a plane normal to the axis of the area intercepted by the cutting plane. Groups of equivalent bodies for different values of θ must be considered to determine drag accurately. Therefore, at each Mach number, a series of equivalent bodies of revolution is generated. The Von Karman slender body formula gives drag as a function of the equivalent body area distribution and free stream conditions. For a given Mach number, the wave drag is taken to be the integrated average of the equivalent body wave drags [2]

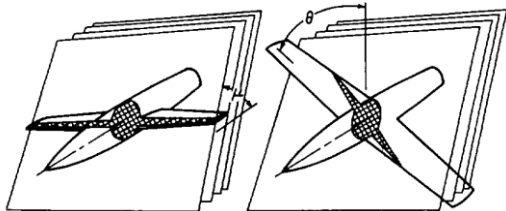


Figure 3 - Projected areas of Mach angle cutting planes intersecting a body [2]

II. HAACK BODIES

The integral equation developed by Von Karman is used for the wave drag calculation of slender bodies of revolution

at various Mach numbers. Haack and other theorists have also used this equation to design various shapes of minimum drag bodies. For any specific set of variables such as length and diameter, length and volume, or diameter and volume, there are specific shapes for minimum drag at some specific Mach numbers for each case. Each is referred to as L-D, L-V, and D-V respectively.

Mathematically, the equations given below describe the revolved profiles.

$$\theta = \arccos\left(1 - \frac{2x}{L}\right) \quad (1)$$

$$y = R(x) = \frac{R}{\sqrt{\pi}} \sqrt{\theta - \frac{\sin(2\theta)}{2} + C \sin^3(\theta)} \quad (2)$$

Where;

L is the overall length of the body

R is the thickness/radius of the body

y is the radius of the body at a particular x location as it varies from one end to the other

The series is a continuous set of shapes determined by the value of C in the equation. C=0 denotes the LD-Haack (Von Karman) which is used in the Harris wave drag code. LD signifies a minimum drag for a minimum length and diameter. While C=1/3 signifies LV-Haack that indicates minimum wave drag for a given length and volume [4]. The values are given as:

Table 1 - Constant Values

	C	C _p
L-V	0.333	0.59
L-D	0	0.519
D-V	-0.666	0.392

Maximum cross-sectional area aids the calculation of maximum radius circular cross-sections. The formula for maximum area is given as:

$$A_{max} = \frac{V}{C_p \cdot L} \quad (3)$$

Following the three Haack Series, different wing-body configurations were formed using the aforementioned equations. All three configurations are shown with the respective cross-sectional area distributions. Figure 4, Figure 5, and Figure 6 show the configurations formed by employing L-D, L-V, and D-V Haack Series formulations respectively. Wave drag analysis has also been carried out on all three configurations and the results are shown in Figure 7, which shows the variation of drag with Mach number. DV Haack optimised geometry has drag significantly lesser than the other two configurations.

Experiments have been carried out to compare the wave drag values of bodies of revolution with optimised shapes derived from the equation above. It is also concluded that with the greater bluntness of the shape of the body, the drag coefficient would increase with increasing Mach number whereas if the bluntness is not significant then the drag coefficient decreases with increasing Mach number over a greater part of the range. Hence, there is no particular shape for the complete Mach range. The study in [3] concludes that if the fineness ratio is constant then blunting is increased that results in a decrease in drag and if the blunting is kept

constant then the fineness ratio is reduced to reduce the drag. A fuselage with a wing of a typical modern fighter aircraft was modelled with the volume of a typical fighter enclosed by the body-wing configuration. For all three series, L-D, L-V, and D-V, certain geometrical parameters were held constant and area ruling was carried out based on the difference in the equation resulting in the shape of the respective optimised bodies.

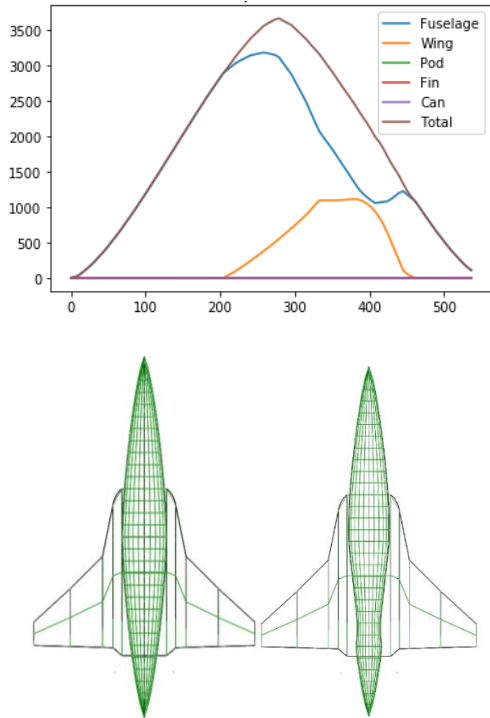


Figure 4 - Left: Initial geometry, Right: L-D Haack optimised geometry, Top: Optimised geometry total area distribution

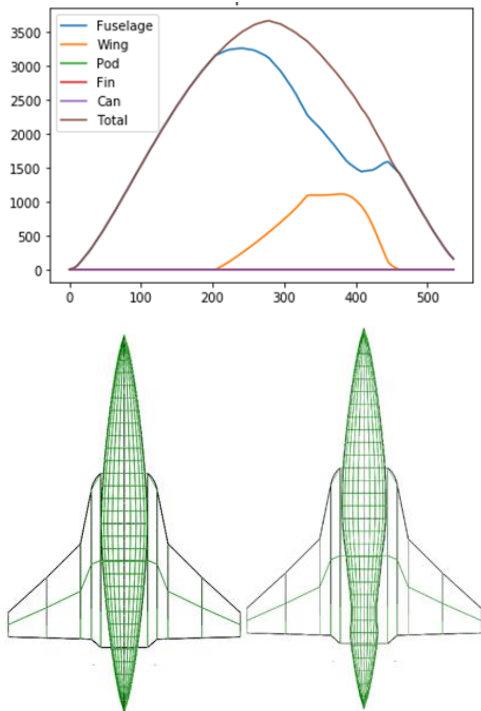


Figure 5 - Left: Initial geometry, Right: L-V Haack optimised geometry, Top: Optimised geometry total area distribution

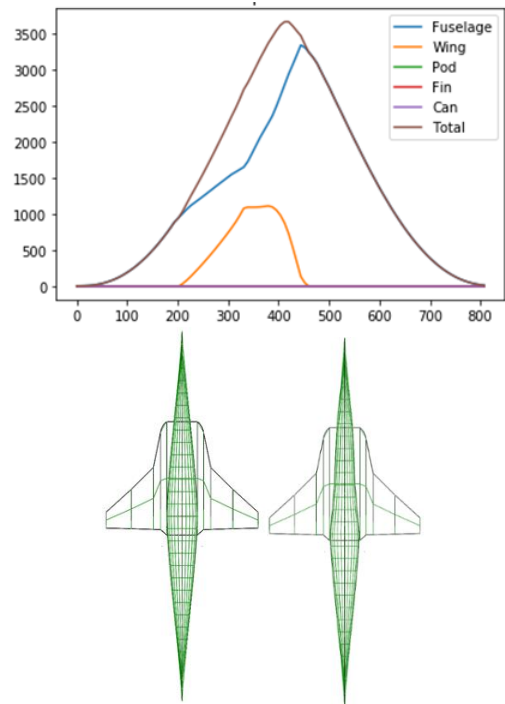


Figure 6 - Left: Initial geometry, Right: D-V Haack optimised geometry, Top: Optimised geometry total area distribution

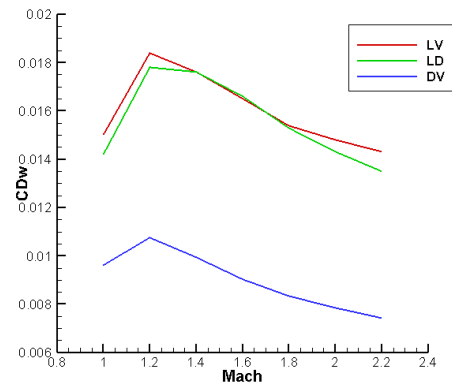


Figure 7 - CDw vs Mach for LD, LV & DV

These three optimised bodies were analysed for a particular range of Mach numbers. Values of wave drag over this range are noted and compared. Hence for the sake of research, the series with the fairest results was selected for the optimisation and analysis of modern fighter aircraft.

Table 2 - C_{Dw} at Mach 1.0 - 1.4 for LV, LD and DV

	LV	LD	DV
C_{Dw} M1.0	0.015	0.014	0.0096
C_{Dw} M1.2	0.0184	0.0178	0.0107
C_{Dw} M1.4	0.0176	0.0176	0.00995

The difference in drag is due to the difference in shapes and bluntness of the three bodies. As shown in the results of the Haack bodies, it can be seen that the L-D and L-V Haack bodies retained the total length of the aircraft, whereas the D-V Haack body has extended length since the parameters that are kept constant are diameter and volume. Since L-D and L-V Haack bodies have lesser bluntness of the overall body that

is the reason why D-V produced minimum wave drag out of all three bodies. Since length extension is a phenomenon not acceptable for fighter aircraft hence using the D-V Haack series to optimise the shape is omitted. Out of the other two bodies, L-D has lesser drag comparatively because L-D has more bluntness towards the nose compared to L-V. Therefore, the series selected is L-D Haack to optimise the shape to minimise the wave drag for better supersonic performance.

III. MATHEMATICAL MODELLING

The wave drag is further split into wave drag due to lift and wave drag due to volume. There are two major approaches to calculate the wave drag of a configuration

- Near-field theory
- Far-field theory

The near-field theory is based on calculating forces by integrating pressure drag acting normal to the surface and tangential stress acting over the surface.

Mathematical modelling of the far-field theory is easy and provides a consistent approach to calculate wave drag of the configuration. In this theory, the drag of the configuration is determined from momentum change through the boundaries of the control volume. The control volume for this approach as shown in Figure 8 is typically cylindrical. Momentum change between the sides S1 and S3 of the control volume is due to the induced drag and the skin friction drag.

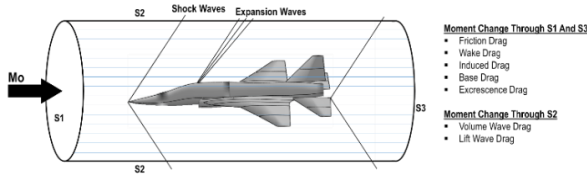


Figure 8 - Representation of the control volume

All sides of the control volume are several body lengths away from the configuration. In the subsonic regime, the flow becomes parallel to sides S2 of the control volume so there is no momentum change across the cylindrical sides S2 of the control volume. In the supersonic regime, momentum change occurs through the cylindrical sides S2 due to shock waves formation by configuration.

Lomax [5] showed that the wave drag of a series of equivalent-volume bodies can be calculated by the momentum change through the cylindrical sides S2 of the control volume. Area distributions of the configuration at each streamwise station can be determined by the projections of oblique cutting planes to the normal planes. These oblique cutting planes are tangent to the Mach cone angle. Tangency angle theta is the rotation of the configuration in the Mach cone or rotation of the cutting plane for fixed configuration. If $\theta = 90^\circ$, the cutting plane is tangent to the top of the Mach cone and momentum change occurs through the top of the control volume. The $\theta = 0^\circ$, cutting plane is tangent to the side of the Mach cone and momentum change occurs through the side of the control volume [6-14].

Drag equation due to total momentum change across the sides of control volume in (5) as:

$$D = \frac{1}{2\pi} \int_0^{2\pi} D(\theta) d\theta \quad (4)$$

$$\iint_{S_3=S_1} (p - p_\infty) \partial S_3 - \rho_\infty U_\infty^2 \iint_{S_3=S_1} \varphi_x (1 + \varphi_x) \partial S_3 - \rho_\infty U_\infty^2 \iint_{S_2} \varphi_x \varphi_r \partial S_2 + \sum D_{misc} = D \quad (5)$$

Due to the S3 side of control volume placed far enough, the flow becomes 2-D and streamwise perturbation velocity is considered zero.

$$\rho_\infty U_\infty^2 \iint_{S_3=S_1} \varphi_x (1 + \varphi_x) \partial S_3 = 0 \quad (6)$$

And the equation is reduced to

$$\iint_{S_3=S_1} (p - p_\infty) \partial S_3 - \rho_\infty U_\infty^2 \iint_{S_2} \varphi_x \varphi_r \partial S_2 = D \quad (7)$$

Wave drag can be calculated directly from velocity change in the side direction as

$$-\rho_\infty U_\infty^2 \iint_{S_2} \varphi_x \varphi_r \partial S_2 = D(\theta) \quad (8)$$

The conventional form of wave drag after a necessary integral operation

$$D(\theta) = -\frac{\rho V^2}{4\pi} \int_0^l \int_0^l S''(x_1) S''(x_2) \text{LOG}|x_1 - x_2| \partial x_1 \partial x_2 \quad (9)$$

Substituting (9) in (4) for angular rotation of cutting planes

$$D = -\frac{1}{2\pi} \frac{\rho V^2}{4\pi} \int_0^{2\pi} \int_0^l \int_0^l S''(x_1) S''(x_2) \text{LOG}|x_1 - x_2| \partial x_1 \partial x_2 d\theta \quad (10)$$

$$\frac{D}{q} = -\frac{1}{4\pi^2} \int_0^{2\pi} \int_0^l \int_0^l S''(x_1) S''(x_2) \text{LOG}|x_1 - x_2| \partial x_1 \partial x_2 d\theta \quad (11)$$

$$S''(x_1) = A''(x_1, \theta) - \frac{\beta}{2q} l'(x_1, \theta) \quad (12)$$

$$S''(x_2) = A''(x_2, \theta) - \frac{\beta}{2q} l'(x_2, \theta) \quad (13)$$

Term $A''(x_1, \theta)$ is the second derivative of equivalent body area distribution due to volume and the term $\frac{\beta}{2q} l'(x_1, \theta)$ is equivalent body area due to lift.

$$\beta = \sqrt{M^2 - 1} \quad (14)$$

Wave drag due to lift approaches to zero as Mach number approaches to 1.

$$\frac{D}{q} = \frac{-1}{4\pi^2} \int_0^{2\pi} \int_0^L \int_0^L \left[A''(x_1, \theta) - \frac{\beta}{2q} l'(x_1, \theta) \right] \left[A''(x_2, \theta) - \frac{\beta}{2q} l'(x_2, \theta) \right] \log_e |x_1 - x_2| dx_1 dx_2 d\theta \quad (15)$$

Jones considered the cases when no lift is generated on aircraft configuration. Then Lomax equation 15 is reduced to

$$\frac{D}{q} = \frac{-1}{4\pi^2} \int_0^{2\pi} \int_0^L \int_0^L [A''(x_1, \theta)] [A''(x_2, \theta)] \log_e |x_1 - x_2| dx_1 dx_2 d\theta \quad (16)$$

Equation 16 is also known as Von Kármán slender body formula which calculates wave drag based upon equivalent area distributions and given free stream conditions.

IV. RESULTS

The selection of the Haack series for our study is determined based on these results. As one would assess, D-V Haack should be the preferable option bearing the least wave drag over the same range of Mach numbers. But in modern fighter aircraft, the length is an important design parameter, and extending the length of a fighter aircraft has its repercussions. Therefore, the option of selecting the D-V Haack is out of the discussion. Among both, L-D and L-V, the selection was clear. Hence, for our study, L-D Haack was selected for attaining the smooth cross-sectional area distribution curve.

The baseline geometry of a modern fighter aircraft is illustrated above in Figure 9. The cross-sectional area plots of the entire geometry, including the fuselage, wing, empennage, and pods are shown in Figure 10. The initial cross-sectional area plot of the entire geometry is shown with every component marked. Fuselage does not have noticeable indentations as area ruling is expected to add to the geometry. Therefore, the total cross-sectional area distribution curve does not follow the smooth Sears Haack area curve which is designed for minimum possible wave drag.

Applying area ruling on the baseline configuration in accordance to L-D Haack has resulted in a smoother overall total cross-sectional area distribution and the difference in wave drag before and after area ruling was applied is visibly clear. The motive of carrying out the optimization of the fuselage shape as per the phenomenon of L-D Haack is fulfilled. The difference in shape, cross-sectional area distribution, and therefore the wave drag is shown.

Fuselage cross-sectional area distribution is also shown in Figure 11. This distribution indicates the indentations that optimization created along the length. This is to accommodate other components and follow the smooth Sears Haack cross-sectional area distribution. Optimized fuselage area distribution is compensating by increasing first and then decreasing afterward, this is because of the reason that in fighter aircraft volume can be comprised but to a certain limit. To accommodate fuel, avionics systems, and weapons in internal bays for stealth, in the case of new generation fighter aircraft, the internal volume of the aircraft can neither exceed a certain nor be lesser than the minimum required value.

Therefore, area ruling with volume conservation using the L-D Haack series is selected and the original configuration as shown in Figure 9 is optimized as shown in Figure 12. Figure 13 shows the cross-sectional area distribution of the optimized geometry and it is evident that the optimized cross-sectional distribution matches the sears Haack distribution and therefore the drop in wave drag as seen in Figure 14.

A significant difference in wave drag of a configuration before and after optimisation can be seen in Table 3, where the wave drag at Mach 1.0, 1.2, and 1.4 are analysed. The percentage difference in the wave drag values at all different Mach numbers for all configurations are also summarised in Tab. 3.

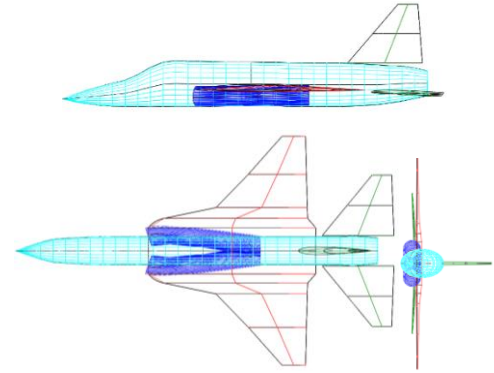


Figure 9 - Initial Geometry

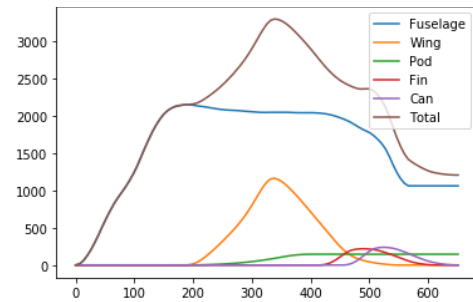


Figure 10 - Initial geometry component-wise cross-sectional area distribution

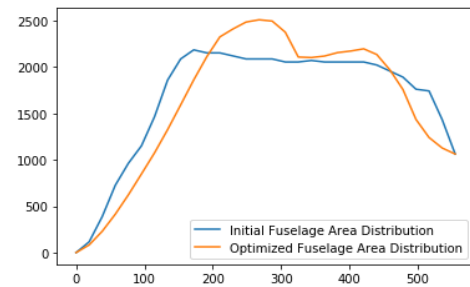


Figure 11 - Fuselage area distribution

Table 3 - C_{Dw} before and after optimisation at different Mach

C_D	Initial Configuration	Optimised Configuration	Percentage Difference
C_{Dw} M1.0	0.039	0.022	38
C_{Dw} M1.2	0.024	0.014	39
C_{Dw} M1.4	0.019	0.015	25

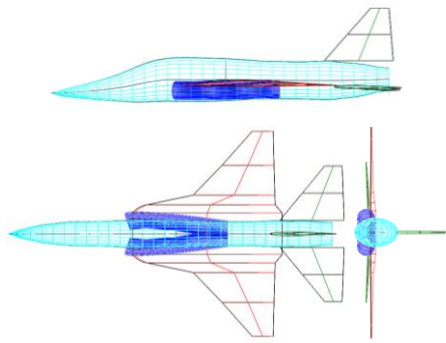


Figure 12 - Optimised Geometry

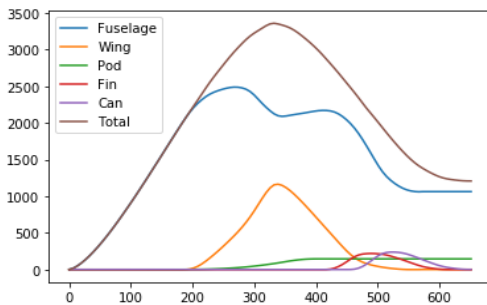


Figure 13 - Optimised geometry component-wise cross-sectional area distribution

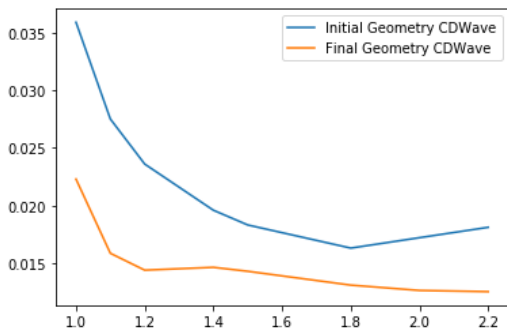


Figure 14 - CD_w vs Mach

Drag polar for both the shapes, with crude area distribution and with a smoother sears Haack type area distribution is shown in Figure 15.

Therefore, a plot of aerodynamic efficiency and coefficient of lift is also shown in Figure 16, representing the improvement in the aerodynamics of the aircraft after area ruling. The improved value of L/D max will lead to better aerodynamic and mission performance.

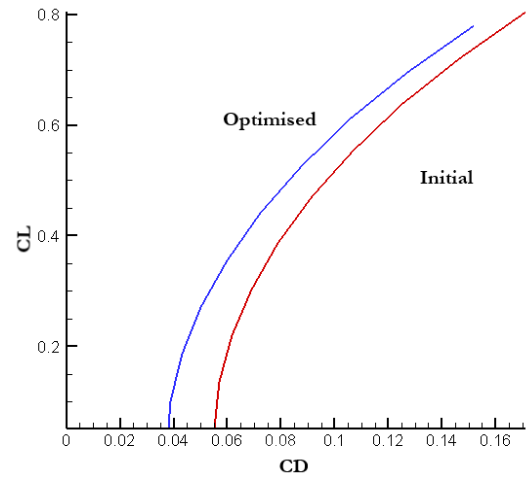


Figure 15 - Initial and optimised geometry drag polar

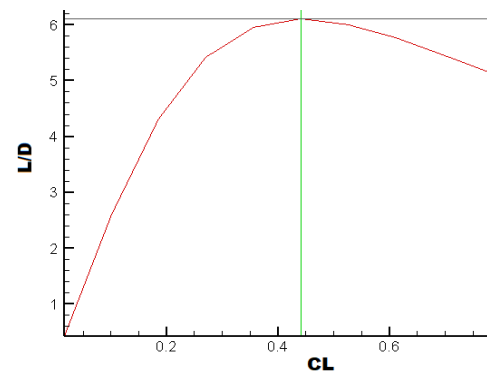


Figure 16 - Optimised geometry drag polar

V. SENSITIVITY ANALYSIS

Other than area ruling, wave drag is sensitive to parameters such as wing sweep, wing thickness, type of aerofoils, flight conditions, etc. For wave drag minimization, the sensitivity of such parameters is studied in the following sections.

A. Sweep

Sweeping the wings delays the supersonic flow. Therefore, as a part of the prospects and continuation of this study, sweep angles variation is analysed from the range of 0° to 60° with results summarised in Table 5 and plotted in Figure 17. The greater the sweep, the greater the critical Mach number, and the formation of shockwaves is stalled.

Table 4 - Variation in CD_w by changing wing sweep for a range of Mach

Sweep Mach	0	10	20	30	40	47	50	60
1	0.039	0.038	0.045	0.045	0.041	0.041	0.041	0.026
1.1	0.031	0.034	0.034	0.034	0.035	0.033	0.035	0.027
1.2	0.028	0.027	0.028	0.028	0.028	0.028	0.028	0.024
1.4	0.022	0.022	0.022	0.022	0.021	0.022	0.021	0.020
1.5	0.021	0.020	0.019	0.019	0.019	0.020	0.019	0.020
1.8	0.017	0.017	0.018	0.018	0.018	0.018	0.018	0.019
2.0	0.019	0.019	0.019	0.019	0.019	0.019	0.019	0.020

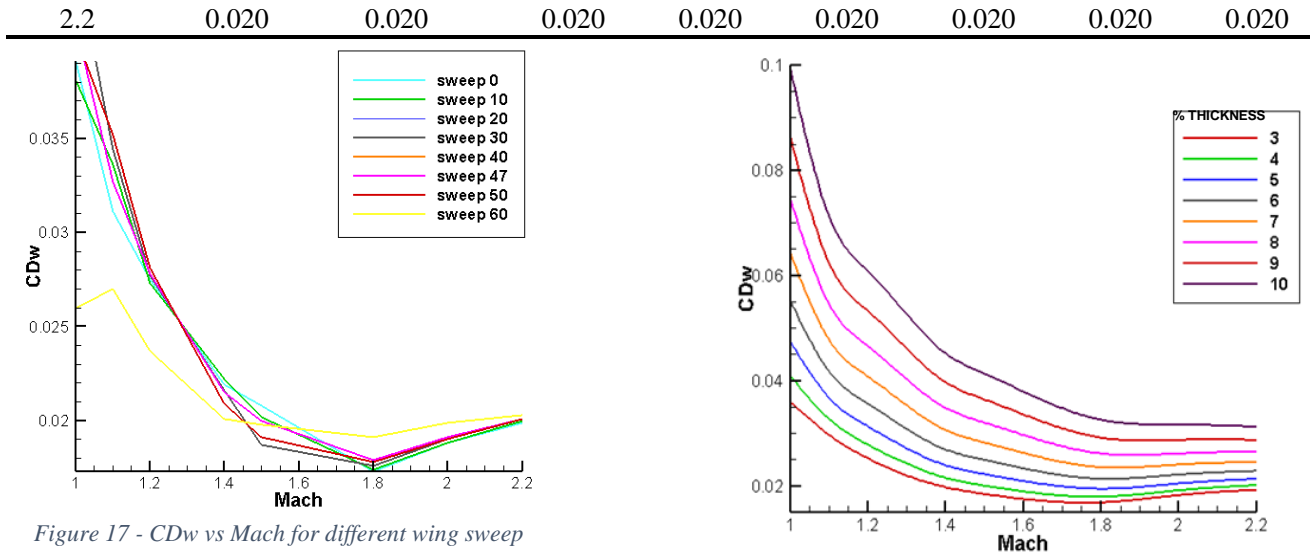


Figure 17 - CDw vs Mach for different wing sweep

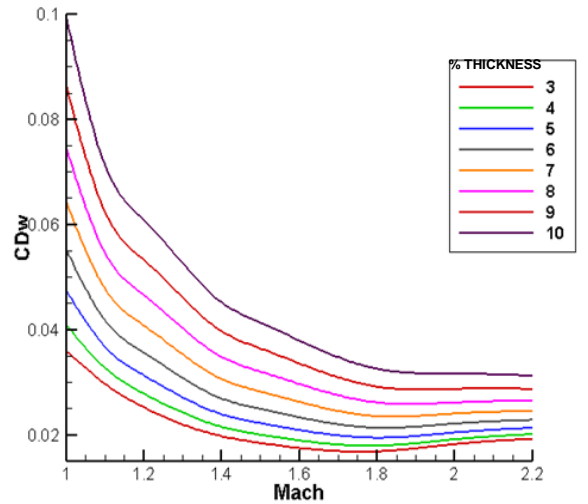


Figure 18 - CDw vs Mach for different thickness

B. Thickness

The thickness of the aerofoil used plays an important part in determining the aerodynamic characteristics of the aircraft. Increasing the thickness of the wing increases the drag of the aircraft due to increased flow separation. As the results have shown the statement is valid that the greater the thickness, the greater the drag. Figure 18 shows that if the aerofoil thickness is

10% then the drag is the highest for the same range of Mach numbers.

Table 5 Variation in CDw by changing wing thickness for a range of Mach

Mach	Thickness								
	3	4	5	6	7	8	9	10	
1	0.036	0.041	0.048	0.055	0.064	0.075	0.086	0.099	
1.1	0.030	0.033	0.037	0.042	0.048	0.055	0.062	0.071	
1.2	0.025	0.028	0.031	0.036	0.041	0.047	0.053	0.061	
1.4	0.020	0.022	0.024	0.027	0.031	0.035	0.040	0.045	
1.5	0.018	0.020	0.022	0.025	0.028	0.032	0.036	0.041	
1.8	0.017	0.018	0.019	0.021	0.024	0.026	0.029	0.033	
2.0	0.018	0.019	0.020	0.022	0.024	0.026	0.029	0.032	

C. Angle of Attack

Flow separation is an important feature determined by the angle of attack of the aircraft. The results are shown in Figure 19 show higher drag at high negative and positive values of angle of attacks.

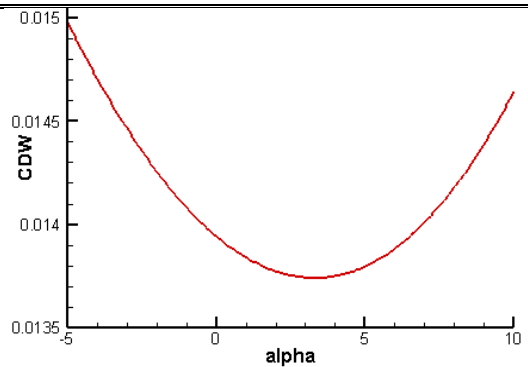


Figure 19 - CDw vs AoA

VI. CONCLUSION

Wave drag causes a significant rise in the total drag as the aircraft approaches supersonic speed. This is the reason why the transition from the subsonic to the supersonic regime is considered one of the most critical segments of the entire flight envelope. Various techniques are incorporated into the design phase of aircraft to reduce the wave drag and therefore enhance high-speed performance.

Shape optimization is one of the core preliminary design phase procedures for reducing the drag penalty. The study explored all three Haack series for a wing-body combination to assess the methodology applicable for the modern multirole fighter shape optimization for the reduction of wave drag. Area ruling is carried out using all three series analytically and the trend of variation in wave drag for all the shapes assisted in the selection of one for the final aircraft body optimization. The analytical equations in the literature for these series are derived for nose cone designs or bullet bodies. For this study, the equations were translated over the entire fuselage and therefore wing-body combinations are derived for each series based on the required total volume of a fighter aircraft configuration as per the requirement.

The wave drag for a wing-body configuration shaped analytically through the L-V Haack series at Mach 1.2 is 0.0184 whereas, for L-D and D-V, the values are 0.0178 and 0.0107 respectively. Although D-V Haack produced minimum drag nonetheless, increased length cannot be an exception in the case of fighter aircraft. Therefore, the L-D Haack series is selected for the fuselage shape optimization and incorporating area ruling into the final shape of the fighter for lesser wave drag.

Wave drag before optimizing the shape of the fuselage was as high as over 0.039 that dropped down to 0.022 after optimization at Mach 1.0 as shown in Table 3 and the difference in overall cross-sectional area elucidates the fact that smoother the area distribution, more of a Sears Haack shape, lesser the wave drag.

Fuselage shape optimization is one of the techniques to counteract the performance deteriorating effects wave drag has on the aircraft in the supersonic regime. With the great advancements in aviation technology, flying at higher Mach numbers is a key design and performance feature for fighter aircraft. As mentioned earlier, super-cruise is one of the highlighting features of next-generation modern fighters, and design must be carried out in a way that substantially increases the super-cruise capabilities.

ACKNOWLEDGMENT

The authors gratefully acknowledge the contributions of Kamran Zeb, M. Arqam, and T. Karim for their assistance on the completion of this study.

REFERENCES

- [1] D. A. Donald and S. K. Ronald, "Wave Drag and High-Speed Performance of Supersonic STOVL Fighter Configurations," NASA, 1988.
- [2] J. Roy V. Harris, "AN ANALYSIS AND CORRELATION OF AIRCRAFT WAVE DRAG," Langley Research Center, 1965.
- [3] P. W. Edward, J. H. Leland and S. C. Simon, "Investigation of The Drag of Various Axially Symmetric Nose Shapes of Fineness Ratio 3 for Mach Numbers from 1.24 to 7.4," National Advisory Committee for Aeronautics, Washington, 1958.
- [4] "Nose cone design," Wikipedia, [Online]. Available: https://en.wikipedia.org/wiki/Nose_cone_design. [Accessed 2018].
- [5] L. Harvard, "The Wave Drag of Arbitrary Configurations In Linearized Flow As Determined By Areas And Forces In Oblique Planes," NACA, Washington, 1955.
- [6] N. Vojin and J. J. Eric, "Zero-Lift Wave Drag Calculations Using Supersonic Area Rule And Its Modifications," in *42nd AIAA Aerospace Sciences Meeting and Exhibit*, Reno, Nevada, 2004.
- [7] C. Citak, S. Ozgen and G. W. Weber, "Mathematical Modelling for Wave Drag Optimization and Design of High-Speed Aircrafts," in *Springer Proceeding in Mathematics and Statistics 195*, Ankara, 2017.

- [8] J. Roskam, "PART VI: PRELIMINARY CALCULATION OF AERODYNAMIC, THRUST AND POWER CHARACTERISTICS," In *AIRPLANE DESIGN*, Lawrence, Kansas, 1987, p. 57.
- [9] K. S. Rallabandi and N. D. Mavris, "An Unstructured Wave Drag Code For Preliminary Design of Future Supersonic Aircraft," *33rd AIAA Fluid Dynamics Conference and Exhibit*, 23-26 June 2003.
- [10] Roy V. Harris, Jr., "27. A Numerical Technique For Analysis of Wave Drag at Lifting Conditions," NASA Langley Research Center.
- [11] M. J. Waddington, "Development of an interactive wave drag capability for the open VSP parametric geometry tool," California Polytechnic State University, San Luis Obispo, 2015.
- [12] G. Xiaohui, "Supersonic Wing-Body Two-Level Wave Drag Optimization Using Extended Far-Field Composite-Element Methodology," *AIAA Journal*, vol. 52, no. 5, pp. 981 - 990, 2014.
- [13] A. Nikita and P. Alexander, "Minimization of body of revolution aerodynamic drag at supersonic speeds," *Aircraft Engineering and Aerospace Technology*, vol. 88, no. 2, 2016.
- [14] K. Brenda, "New Supersonic Wing Far-Field Composite-Element Wave-Drag Optimization Method," *Journal of Aircraft*, vol. 46, no. 5, pp. 1740 - 1758, 2009.